

Received June 10, 2019, accepted June 19, 2019, date of publication June 24, 2019, date of current version July 11, 2019.

Digital Object Identifier 10.1109/ACCESS.2019.2924515

# Research on the Steady Operation Optimization Model of Natural Gas Pipeline Considering the Combined Operation of Air Coolers and Compressors

ENBIN LIU<sup>1</sup>, LIUXIN LV<sup>1,2</sup>, YANG YI<sup>1,3</sup>, AND PING XIE<sup>4</sup>

<sup>1</sup>Petroleum Engineering School, Southwest Petroleum University, Chengdu 610500, China

<sup>2</sup>Kunshan Litong Natural Gas Company Ltd., Kunshan 215300, China

<sup>3</sup>Sinopec Xinjiang Coal-to-Gas Natural Gas Pipeline Company Ltd., Beijing 100020, China

<sup>4</sup>PetroChina Northwest United Pipeline Company Ltd., Urumqi 830001, China

Corresponding author: Enbin Liu (enbin.liu@swpu.edu.cn)

This work was supported in part by the Sichuan Provincial Applied Basic Research Project under Grant 2019YJ0352 and in part by the Sichuan Provincial Natural Resources Research Project under Grant KJ-2019-11.

**ABSTRACT** Based on the mutual coupling effect among the compressor, the air cooler and pipes in the system of natural gas pipeline, innovatively with the goal of minimum energy consumption, this paper established a combined operation optimization model of the air cooler and compressor through the optimization of the switching scheme of compressors and air coolers, which can greatly reduce the production energy consumption of the pipeline system. Moreover, when the air temperature is taken as an optimization variable, the most proper temperature to start the air cooler of each compressor station can be worked out to guide the optimized operation of the pipeline, which is of high value for promotion and application. The case analysis of west-east natural gas pipeline II showed that among genetic algorithm (GA), particle swarm optimization (PSO), and simulated annealing (SA) algorithm that are used to solve the optimization model, the genetic algorithm is the fastest, and the simulated annealing algorithm the slowest, but the optimization results of the simulated annealing algorithm is the best, in which the reduced production energy consumption accounted for 33.77%, testifying the practicability and creativity of the optimization model.

**INDEX TERMS** Natural gas pipeline, air cooler, compressor, operation optimization, algorithm.

## I. INTRODUCTION

In the long-distance natural gas pipeline, the air cooler is often installed at the compressor outlet of the compressor station. When the outlet temperature of the compressor is high, it is necessary to use air cooler to cool down the natural gas, causing the reduction of the viscosity of natural gas, the volume flow, the operating noise and the friction loss [1], thus increasing the inlet pressure of the next compressor station, lowering the compression ratio of the compressor, and consequently reducing the energy consumption of the compressor set [2]. However, in the process of pipeline operation optimization, existing researchers tend to only take the energy consumption of the compressor into account but ignore the influence of the air cooler on the energy consumption of the compressor or

even the whole pipeline system. In 2015, Xie *et al.* [3] made a comparison among switching schemes of air coolers in three compressor station through the determination of the outlet temperature of compressor station, to compare the energy consumption of compressor stations. However, in terms of the long natural gas pipeline, the number of compressor stations is large, and the pipeline mileage is long, so it is not possible to draw a conclusion only by comparing the schemes. Therefore, it is necessary to establish an operation optimization model of the pipeline including air coolers. The research on optimization model and calculation mainly includes the following four aspects:

(1) Objective function: in the operation optimization of the natural gas pipeline, Chi *et al.* [4] took the maximum gas volume as the objective function; Liu *et al.* [5], [6] took the minimum energy consumption as the objective function; Demissie *et al.* [7] and Ghoujdi *et al.* [8] took the maximum

The associate editor coordinating the review of this manuscript and approving it for publication was Kuo-Ching Ying.

economic benefit as the objective function. The most widely used is the optimization model of minimum energy consumption. However, the optimization model established by previous studies never took the influence of the energy consumption of air coolers into consideration. This paper innovatively added the energy consumption of air coolers into the objective function to establish the combined operation optimization model of air coolers and compressors with the minimum total energy consumption of pipelines as the objective function.

(2) Optimization variables: They usually include the pressure and temperature of each joint, the flow of each unit (pipes and compressors), the condition and power of each compressor, among which, the pressure, flow and compressor power are continuous variables. Roger and Conrado [9] and Kody and Xiang [10] considered the condition of compressor as discrete variable. This paper, on the basis of the previous research, takes the number of power-on air coolers as an optimization variable as well.

(3) Constraints: Liu *et al.* [5], [6] used the inequality constraints to limit the flow, pressure and temperature of the pipeline within a specified range. In addition, the economic constraints for starting air coolers should be considered [11]. Equation constraints mainly represent the control equations of gas flowing in pipelines, including mass balance equation, pressure equation and temperature equation [12]. Compressor constraints were firstly established on the basis of the assumption of the ideal compressor without combining with the actual working condition. Suming *et al.* [13] and Liu *et al.* [5], [6] established a set of polynomials including surge curve and stagnation curve, to describe the feasible domain of the compressor, obtaining the constraints that accord with the actual operation of compressors. At the same time, the operation of compressors should satisfy their own constraints of rotating speed [14]. Moreover, the power constraints of the air cooler are also taken into consideration in this paper.

(4) Optimization algorithm: Goldberg [15], for the first time, applied genetic algorithm [16] to solve the operation optimization problem of natural gas pipeline. Sanaye and Mahmoudimeh [17] used genetic algorithm to solve the optimization problem of natural gas pipeline network. Kennedy [18] proposed particle swarm optimization in 2010. Li *et al.* [19]–[22] used particle swarm optimization to find out the minimum energy consumption of natural gas pipeline network. Kirkpatrick *et al.* [23] proposed simulated annealing algorithm in 1979, but simulated annealing algorithm was not applied to the operation optimization of natural gas pipelines until 2007 [24]. Dorigo proposed the ant colony algorithm in 1992. Chebouba *et al.* [25] were the earliest to use the ant colony algorithm to solve the operation optimization problem of natural gas pipeline and in 2012, based on the steady-state assumption, the number of compressors and outbound pressure of a natural gas pipeline system were optimized [26]. Wu *et al.* [27] applied the differential evolution to the research on operation optimization of

the pipeline including 11 pipelines and 2 compressor stations. When vector machines and artificial neural networks [28], [29] are supported to solve the operation optimization of the pipeline, other optimization algorithms are usually used in combination. Borraz-Sánchez and Ríos-Mercado [30] proposed a hybrid discontinuous dynamic programming and taboo search method to solve the operation optimization of the natural gas pipeline. Wong and Larson [31], in 1968, for the first time, used dynamic programming to solve the operation optimization model of the natural gas pipeline. Later on, Danilovic *et al.* [32], Behrooz and Boozarjomehry [33] and Liu *et al.* [5], [6] all successfully applied the dynamic programming. At present, there are quite a few algorithms which have been used to solve the operation optimization of the natural gas pipeline, but the problem is that only compressors are taken into account in the solving process. In this paper, the coupling relationship between the air cooler, the compressor and the pipeline is considered in the solving process, which greatly increases the solving difficulty.

In summary, the existing research results do not consider the influence of air coolers. In this paper, the air cooler is introduced into the natural gas pipeline operation optimization model, and the air cooler related performance constraints are added. An optimization model for the combined operation of air cooler and compressor is established with the aim of minimizing the total energy consumption of pipelines. The operation optimization model is solved by genetic algorithm, particle swarm optimization algorithm and simulated annealing algorithm. The optimal air cooler and compressor startup scheme which can greatly reduce energy consumption are proposed. In addition, this paper also innovatively proposes to use the ambient temperature as an optimization variable to obtain the optimum temperature for opening the air cooler in different seasons. These two tasks have important economic significance for energy saving and consumption reduction of long-distance pipelines.

## II. MODELS AND METHODS

### A. OBJECTIVE FUNCTION

In this paper, the minimum sum of the energy consumption of the compressor set and the air cooler set is taken as the objective function, and the optimization model is established based on the following basic assumptions: (1) the gas flow in the pipeline is in a steady state; (2) the flow in each compressor of each compressor station is equal; (3) the flow in each air cooler is equal. The technological process of the compressor set and the air cooler set is shown in Figure 1. We use the notations listed in Figure 1 throughout this paper.

$$\min F = \min \sum_{i=1}^n (F_{ic}(P_{id}, c_i) + F_{ia}(a_i)) \quad (1)$$

In which:  $F$ – The total energy consumption of compressor stations along the pipeline, tce;

$F_{ic}$ – The energy consumption of the No. $i$  compressor set of the compressor station, tce;

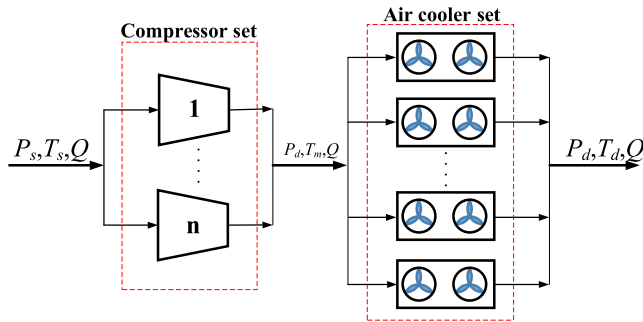


FIGURE 1. Technology flow diagram of the compressor and the air cooler.

$F_{ia}$  – The energy consumption of the No.  $i$  air cooler set of the compressor station, tce;  
 $n$  – The number of the compressor set;  
 $P_{id}$  – The outlet pressure of the No.  $i$  compressor station, MPa;  
 $c_i$  – The number of power-on compressors of the No.  $i$  compressor station;  
 $a_i$  – The number of power-on air coolers of the No.  $i$  compressor station.

**B. OPTIMIZATION VARIABLES**

After turning on the air cooler, the outbound temperature of the compressor station drops, and the subsequent friction resistance of pipeline drops with it, which leads to the increase of the outbound pressure of the next compressor station, the drop of the energy head supplied by the compressor, and the changing of the outbound pressure of the compressor station. Moreover, there is a direct relation between the outbound temperature of the compressor station and the number of power-on air coolers, and the latter could more directly reflect the energy consumption of the air cooler. Therefore, the outbound pressure of the compressor station, the number of power-on compressors and the number of power-on air coolers are taken as optimization variables.

$$X_i = (P_{id}, c_i, a_i) \tag{2}$$

In which:  $P_{id}$  – The outbound pressure of the No.  $i$  compressor station, MPa;

$c_i$  – The number of power-on compressors of the No.  $i$  compressor station;

$a_i$  – The number of power-on air coolers of the No.  $i$  compressor station.

**C. CONSTRAINTS**

1) PRESSURE CONSTRAINTS

The pressure of pipe joint shall satisfy:

$$P_{imin} \leq P_i \leq P_{imax} \quad (i = 1, 2, \dots, N_n) \tag{3}$$

In which:  $P_i$  – The pressure of the No.  $i$  joint, MPa;

$P_{imin}$  – The minimum allowed pressure of the No.  $i$  joint, MPa;

$P_{imax}$  – The maximum allowed pressure of the No.  $i$  joint, MPa;

$N_n$  – Pipe joint.

2) CONSTRAINTS OF PIPELINE STRENGTH

In order to ensure the safe operation of the pipeline, the gas pressure of the No.  $k$  pipe shall satisfy the constraints of pipeline strength:

$$P_k \leq P_{kmax} \quad (k = 1, 2, \dots, N_p) \tag{4}$$

In which:  $P_k$  – The gas pressure of the No.  $k$  pipe, MPa;

$P_{kmax}$  – The maximum allowed pressure of the No.  $k$  pipe, MPa;

$N_p$  – The number of pipes.

3) CONSTRAINTS OF FLOW CONSERVATION

According to the law of conservation of mass, at any joint of the pipeline, the mass of natural gas flowing into the joint should be equal to that out of the joint [6].

$$\sum_{\substack{k \in C_i \\ i = 1}}^{N_n} \alpha_{ik} M_{ik} + Q_i = 0 \tag{5}$$

In which:  $C_i$  – The collection of elements that connect to the No.  $i$  joint;

$M_{ik}$  – The absolute value of the flow of the No.  $i$  joint, into (out of) which the element  $k$  connected to the No.  $i$  joint flows,  $m^3$ ;

$Q_i$  – The flow that the No.  $i$  joint exchanges with the outside;

$\alpha_{ik}$  – Coefficients. When the element  $k$  flows into the joint  $i$ , the  $\alpha_{ik}$  is +1, and when the element  $k$  flows out of the joint  $i$ , the  $\alpha_{ik}$  is -1.

4) THE PIPELINE'S PRESSURE EQUATION

The pipeline's pressure equation describes the relationship between the gas flow rate and pressures at inlet and outlet of the pipeline. The equation is derived from the one-dimensional momentum conservation equation. It takes the following form [35]:

$$M_j = \frac{\pi}{4} \sqrt{\frac{[P_{Qj}^2 (1 - C_1 \Delta h) - P_{Zj}^2] D^5}{\lambda ZRT_{cp} L \left(1 - \frac{C_1 \Delta h}{2}\right)}} \quad (j = 1, 2, \dots, N_n) \tag{6}$$

$$C_1 = \frac{2g}{ZRT_{cp}} \tag{7}$$

In which:  $P_{Qj}$  – The  $j$ th pipe's inlet pressure, Pa;  $P_{Qj}$  is equal to compressor outlet pressure.

$P_{Zj}$  – The  $j$ th pipe's outlet pressure, Pa;  $P_{Zj}$  is equal to compressor inlet pressure.

$M_j$  – The mass flowrate in the  $j$ th pipe, kg/s;

$T_{cp}$  – The pipe's average temperature, K;

$L$  – The pipe length, m;  
 $D$  – The internal diameter, m;  
 $\Delta h$  – The elevation difference between the inlet and outlet of the pipe, m;  
 $g$  – The gravity acceleration, 9.8 m/s<sup>2</sup>;  
 $R$  – The gas constant, 8.314 J/(mol·K);  
 $\lambda$  – The friction factor, which can be calculated by the ColebrookeWhite correlation:

$$\frac{1}{\sqrt{\lambda}} = -2\lg\left(\frac{k}{3.7D} + \frac{2.51}{Re\sqrt{\lambda}}\right) \quad (8)$$

In which:  $k$ – The absolute roughness of the pipe’s internal wall, m;

$Re$  – The Reynold number.

Based on the environment temperature and the inlet temperature, the average temperature  $T_{cp}$  can be calculated by Eq. (9) [42]–[45]

$$T_{cp} = T_0 + (T_Q - T_0) \frac{1 - e^{-\beta L}}{\beta L} - D_i \frac{P_Q - P_Z}{\beta L} \left[ 1 - \frac{1}{\beta L} (1 - e^{-\beta L}) \right] \quad (9)$$

$$\beta = \frac{K\pi D}{MC_p} \quad (10)$$

$$D_i = \frac{1}{C_p} \left[ T \left( \frac{\partial V}{\partial T} \right)_p - V \right] \quad (11)$$

In which:  $C_p$ – The specific heat capacity of the gas, J/(kg·K);  
 $T_Q$ –The temperature at the pipe’s inlet node, K;  
 $T_0$  – The environment temperature, K;  
 $P_Q$ – Starting point pressure, MPa;  
 $P_Z$ – End point pressure, MPa;  
 $K$ – The pipe’s overall heat transfer coefficient, W/(m<sup>2</sup>·K);  
 $D_i$  –Joule-thomson coefficient, °C/Pa;  
 $V$ – Specific volume, m<sup>3</sup>/kg;  
 $\rho$ – Density, kg/m<sup>3</sup>.

$Z$  is the compressibility factor, which can be obtained by equation of state. In this paper, PR state equation is used to calculate the compression factor, and the calculation formula is as follows [35]:

$$Z^3 - (1 - B)Z^2 + (A - 3B^2 - 2B)Z - (AB - B^2 - B^3) = 0 \quad (12)$$

$$A = \frac{aP}{R^2T^2} \quad (13)$$

$$B = \frac{bP}{RT} \quad (14)$$

For a single component

$$a = 0.45724 \frac{R^2T_c^2}{P_c} \alpha \quad (15)$$

$$b = 0.07780 \frac{RT_c}{P_c} \quad (16)$$

$$\alpha^{0.5} = 1 + (1 - T_r^{0.5}) (0.37464 + 1.5422\omega - 0.26992\omega^2) \quad (17)$$

For the mixture of natural gas components

$$a = \sum_i \sum_j y_i y_j (a_i a_j) (1 - K_{ij}) \quad (18)$$

$$b = \sum_i y_i b_i \quad (19)$$

In which:  $T$ – Natural gas temperature, K;  
 $T_c$ – Natural gas critical temperature, K;  
 $T_r$ – Natural gas contrast temperature, K;  
 $P$ – Natural gas pressure (absolute pressure), MPa;  
 $P_c$ – Natural Gas critical pressure, MPa;  
 $P_r$ – Natural gas contrast pressure, MPa;  
 $y_i$ – The mole fraction of component  $i$ ;  
 $K_{ij}$ –The interaction coefficient between  $i$ - $j$  components ( $K_{ij} = K_{ji}$ );  
 $\omega$ –Eccentric factor.

### 5) CONSTRAINTS OF THE PERFORMANCE OF AIR COOLERS *a: THE POWER OF THE AIR COOLER*

The fan of the dry air cooler is the most important energy consuming component, which is driven by the motor, and utilizes the rotation of large blades to accelerate the cold air flow to cool down the hot fluid in the finned tube. The calculation of fan power is equal to the calculation of the operating power of the air cooler.

$$N = 1.35 \times 10^{-7} \bar{N} D^5 n^3 \quad (20)$$

In which:  $N$ – The power of fan shaft, KW;  
 $\bar{N}$  – The shaft power coefficient. The figure is referred to the literature [35];  
 $D$  – Impeller diameter, m;  
 $n$  – The rotating speech of fan, rad/min.

### *b: THE OUTLET TEMPERATURE OF THE AIR COOLER*

The calculation formula of the mean temperature difference of dry air cooler is as follow [34]:

$$\Delta t_{mc} = \frac{(T_1 - t_2) - (T_0 - t_0)}{\ln \frac{T_1 - t_2}{T_0 - t_0}} \quad (21)$$

In which:  $\Delta t_{mc}$ – Log mean temperature difference of the dry air cooler, °C;  
 $T_1$ – Inlet temperature of gas in the finned tube of the dry air cooler, °C;  
 $T_0$ – Outlet temperature of gas in the finned tube of the dry air cooler, °C;  
 $t_0$ – Inlet temperature of the air at the finned tube bundle of the dry air cooler, °C;  
 $t_2$ – Inlet temperature of the air at the finned tube bundle of the dry air cooler, °C.

The author, in the literature [34], [35], established a CFD model, simulated the relation between the difference of inlet and outlet temperature of air cooler, and fitted the results into

the following form:

$$\begin{aligned} \Delta T = & e_1 + e_2n + e_3 (T_{aircoolerin} - T_{air}) \\ & + e_4n (T_{aircoolerin} - T_{air}) \\ & + e_5n^2 + e_6 (T_{aircoolerin} - T_{air})^2 \end{aligned} \quad (22)$$

$$T_{aircoolerout} = T_{aircoolerin} - \Delta T \quad (23)$$

In which:  $\Delta T$ –The temperature drop of natural gas after cooling by the air cooler, K;

$T_{aircoolerout}$  – The temperature of gas at the outlet of the air cooler, K;

$T_{aircoolerin}$  – The temperature of gas at the inlet of the air cooler, K;

$T_{air}$  – The air temperature, K;

$n$  – The number of power-on air coolers.

The adopted value for  $e_1, e_2, e_3, e_4, e_5, e_6$  are as shown in Table 1.

**TABLE 1. Coefficients.**

$e_1$	$e_2$	$e_3$	$e_4$	$e_5$	$e_6$
-2.0388	0.6696	0.0986	0.0302	-0.039	0.0003

#### c: CONSTRAINTS OF APPROACH TEMPERATURE DIFFERENCE

fluid gas and the inlet temperature of cold fluid gas. The approach temperature difference of the air cooler generally requires more than 15° C [11], otherwise it is uneconomical.

$$T_{id} - T_{i0} \geq 15 \quad (24)$$

In which:  $T_{id}$  - The outlet temperature of the air cooler, K;

$T_{i0}$  - The inlet air temperature of the air cooler, K.

#### 6) CONSTRAINTS OF THE PERFORMANCE OF THE COMPRESSOR [6]

##### a: THE COMPRESSOR POWER

$$N = \frac{MH}{\eta} \quad (25)$$

In which:  $N$  – The compressor power set, kW;

$H$  – Polytropic head of the compressor, kg·m/kg;

$M$  – The ratio of the mass of natural gas to the gas flow, kg/s;

$\eta$ - The compressor power.

##### b: THE CURVE EQUATION OF THE COMPRESSOR HEAD

$$-H = h_1S^2 + h_2SQ + h_3Q^2 \quad (26)$$

In which:  $h_1, h_2, h_3$ – Fitting coefficients of head curve;

$S$  – The rotating speed of the compressor, rpm;

$Q$  – The flow of the compressor, m<sup>3</sup>/d.

##### c: THE POWER CURVE EQUATION OF THE COMPRESSOR

$$-H/\eta = e_1S^2 + e_2SQ \quad (27)$$

In which:  $e_1, e_2$ – Fitting coefficients of power curve;

$\eta$ – Polytropic efficiency.

##### d: THE SURGE CURVE EQUATION OF THE COMPRESSOR

$$Q_{surge} = s_1 + s_2H \quad (28)$$

In which:  $s_1, s_2$ - Fitting coefficients of surge curve.

##### e: THE STAGNATION CURVE EQUATION OF THE COMPRESSOR

$$Q_{stone} = s_3 + s_4H \quad (29)$$

In which:  $s_3, s_4$ - Fitting coefficients of stagnation curve.

The above equations are employed to fit the performance curve of the compressor shown in Figure 2 to obtain the coefficients of the equation  $h_1, h_2, h_3, e_1, e_2, s_1, s_2, s_3, s_4$  °

#### 7) THE COMPRESSOR'S TEMPERATURE EQUATION

The temperature of the natural gas also changes with the compression of the gas. The temperature change across the compressor can be calculated by Eq. (28) [35]:

$$T_d = T_s \varepsilon^{\frac{m-1}{m}} \quad (30)$$

In which:  $T_d$ –the discharge temperature, K.

$T_s$ – The suction temperature, K;

$\varepsilon$ – Compression ratio;

$m$ –Polytropic index.

#### 8) CONSTRAINTS OF COMPRESSOR POWER

The operation of the compressor shall satisfy the following power requirements [6]:

$$N_{min} \leq N \leq N_{max} \quad (31)$$

In which:  $N_{min}$ –The minimum allowed power of the compressor, MW;

$N_{max}$ – The maximum allowed power of the compressor, MW.

#### 9) CONSTRAINTS OF THE ROTATING SPEED OF THE COMPRESSOR

The rotating speed of the compressor should be adjusted between the maximum and minimum rotating speed [6].

$$S_{min} \leq S \leq S_{max} \quad (32)$$

In which:  $S_{min}$ –The minimum rotating speed of the compressor, rad/min;

$S_{max}$ – The maximum rotating speed of the compressor, rad/min.

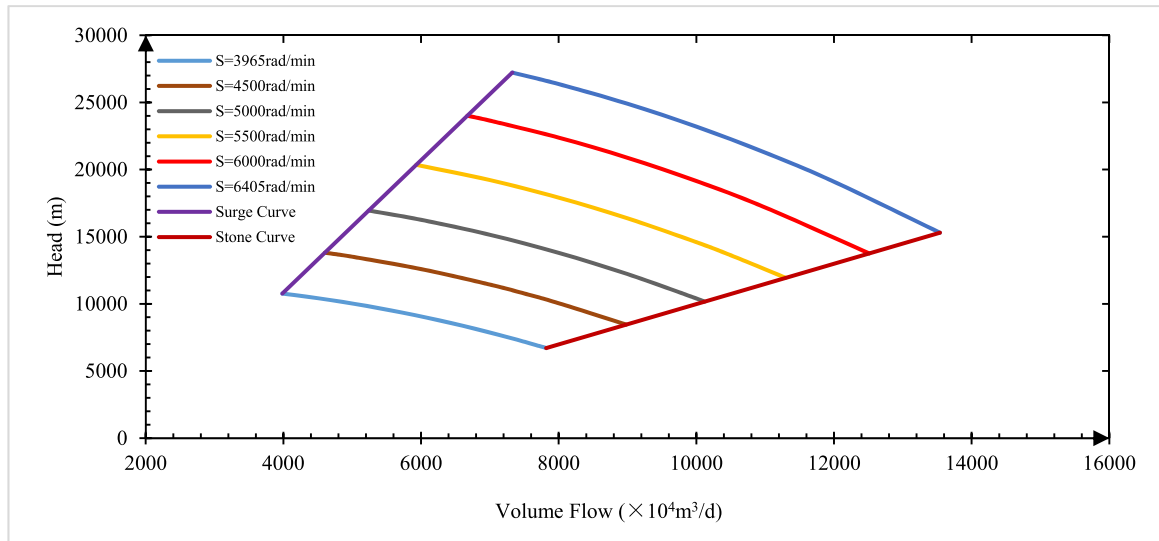


FIGURE 2. Working area of the compressor in Horgos compressor station.

10) CONSTRAINTS OF THE OUTLET TEMPERATURE OF THE COMPRESSOR

The outlet temperature of the compressor, namely the outlet temperature of the air cooler, shall not exceed the following temperature constraints [6].

$$T_m < T_{m \max} \tag{33}$$

In which:  $T_m$ —The outlet temperature of the compressor, K;  
 $T_{m \max}$ — The maximum outlet temperature of the compressor, K.

D. OPTIMIZATION ALGORITHM

The methods for solving the optimal operation model of the natural gas pipeline can be considered mature. Based on Matlab software programming, this research employs the optimal solver and adopts GA [35], PSO [36]–[38] and SA [39]–[41] to solve the model, so as to evaluate the strengths and weaknesses of such algorithms. The key parameters of these algorithms are determined as follows.

1) GA

Genetic algorithm (GA) has a wide range of applications in solving linear programming, stochastic programming, unconstrained optimization, interval programming, and target planning, as it can be processed for any form of objective function and constraints. The core content of the basic genetic algorithm includes four operations of elimination, crossover, mutation and copy. For the actual optimization problem, the following steps can generally be used to solve:

- a. Establish an optimization model and its mathematical expressions to determine the objective function;
- b. Determine the optimization variables and a series of constraints;
- c. Determine a method for calculating individual fitness;

d. Determine the relevant operational parameters of the genetic algorithm evolution process, that is, determine the population size of the genetic algorithm, the termination condition of the algorithm, the crossover probability, the mutation probability and other parameters.

Genetic algorithm solution flow chart shown in Figure 3.

In the evolution process, the population size is set at 60 with crossover probability at 0.8 and mutation probability at 3%. The termination criterion is the maximum evolution algebra 400.

2) PSO

Particle Swarm Optimization (PSO) is a method based on the foraging process of bird populations to find optimized paths under the coordination of groups. In the particle swarm optimization process, each optimization problem is treated as a particle, and an adaptive value is determined by the optimization function in the search space to determine the state of the particle at this position. Each particle can find an optimized position and speed with memory in a certain position, determining the direction and distance of the next step.

The bird is abstracted into particles (points) without mass and volume, and extended to the N-dimensional space. The position of the particle I in the N-dimensional space can be represented by the vector  $X_i = (x_1, x_2, \dots, x_N)$ , and the flying speed can be represented by the vector  $V_i = (v_1, v_2, \dots, v_N)$ . Each particle has a fitness value, and the fitness value is determined by the objective function. In addition, it knows the best position (pbest) that it has found so far and the current position  $X_i$ , which can be considered as a particle. Individual flight experience. In addition, each particle also knows the best position for all particles found in the entire population (gbest, gbest is the best value in pbest), which can be considered as the flying experience of particle companions. Particles

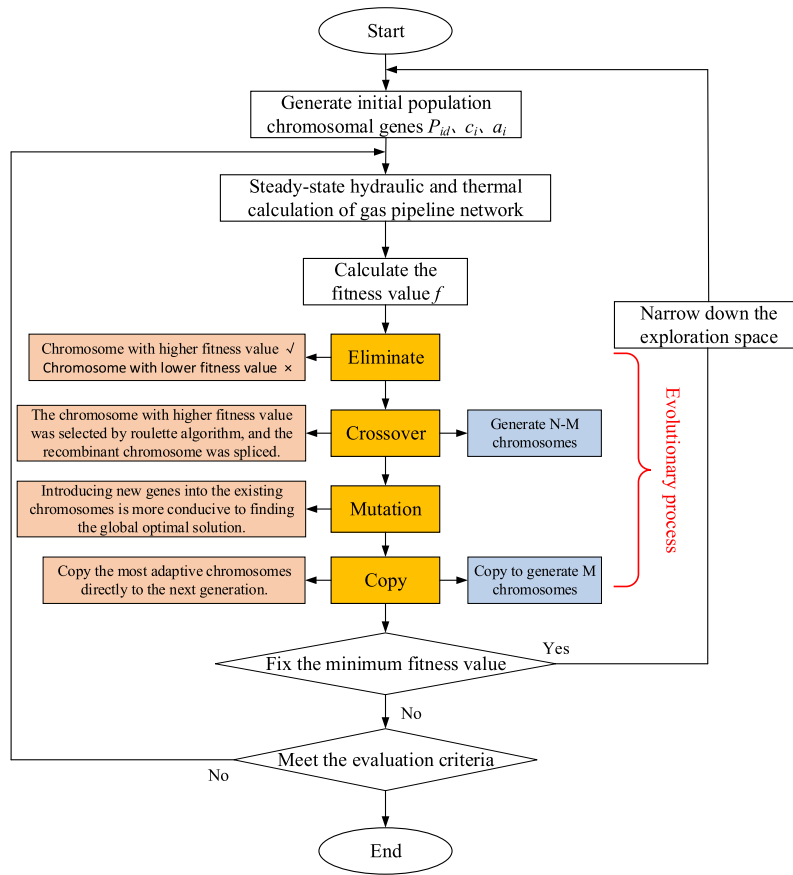


FIGURE 3. GA solution flow chart.

are based on their own experience and the best experience of their peers to determine the next move, and gradually find the global optimal solution.

Particle Swarm Optimization algorithm solution flow chart shown in Figure 4.

Take 40 particles with particle length at 42, then set the maximum speed at 15% of the variation range of each dimension variable and set the acceleration coefficient at 2.0.

### 3) SA

Simulated Annealing(SA) algorithm is derived from the principle of solid annealing. It is a probability-based algorithm that warms the solid to a sufficiently high temperature and then slowly cools it. When heating, the solid internal particles become disordered with temperature rise, and the internal energy increases. Large, and slowly cooling particles gradually become ordered, reaching equilibrium at each temperature, and finally reaching the ground state at normal temperature, the internal energy is reduced to a minimum. The simulated annealing algorithm adds random factors to the search process. In the process of searching, the simulated annealing algorithm will accept a value that is worse than the current solution under a certain probability, so there will be a certain probability to jump out of the local optimal solution,

thus finding the global optimal solution and improving the global search ability.

The basic flow of the simulated annealing algorithm is as follows:

a. Initialize, randomly generate a set of initial solutions,  $i \in S$ , given the initial temperature  $T_0$ , set the termination temperature to  $Tend$ , and make the initial value of the iteration index  $k = 0, T_k = T_0$ ; (Note:  $T_0$  should be large enough to make  $\Delta F/T_k \rightarrow 0$ )

b. Randomly generate a neighborhood solution,  $j \in N(i)$  ( $N(i)$  representing the neighborhood of  $i$ ), and calculate the increment of the objective function,  $\Delta F = F_2 - F_1$ ;

c. If  $\Delta F < 0$ , then let 1 = 2, go to step d (2 better than 1 is unconditional transfer); otherwise, generate  $\xi \in U(0, 1)$ , if  $\exp(-\Delta F/T_k) > \xi$ , then let 1 = 2 (1 is better than 2, transfer under certain acceptance probability conditions).

d. If the number of internal cycles is greater than  $n(T_k)$ , go to step 5, otherwise go to step 2.

e. Let  $k = k + 1$ , reduce  $T_k$  by cooling method, if  $T_k < Tend$  ends the loop, otherwise go to step 2. There are two methods to reduce  $T_k$ , Method 1:let  $T_{k+1} = T_k \cdot q$ , where  $q \in (0.95, 0.99)$ ; Method 2:let  $T_{k+1} = T_k - \Delta T$ . In this paper, method 1 is adopted to reduce  $T_k$ , which is simple and feasible.

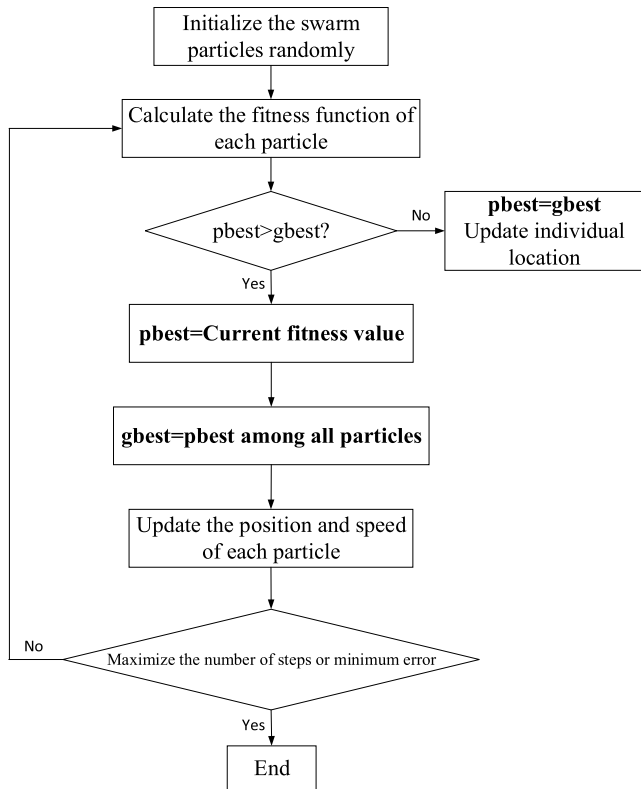


FIGURE 4. PSO solution flow chart.

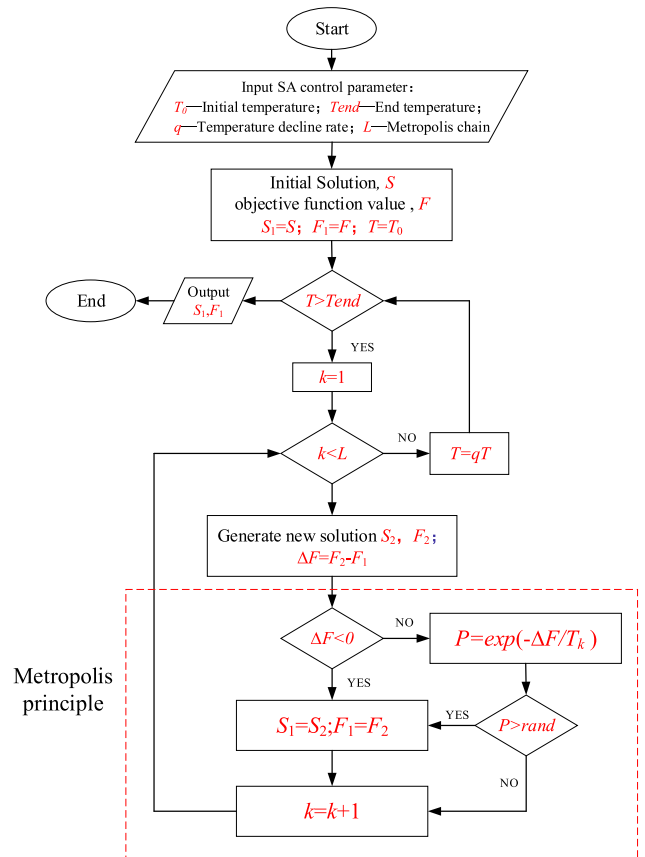


FIGURE 5. SA solution flow chart.

Simulated Annealing algorithm solution flow chart shown in Figure 5.

The initial temperature is 100, ending with 0.001. The cooling factor is set at 0.98.

### III. RESULTS AND DISCUSSIONS

#### A. OPTIMIZATION CASE

A large natural gas pipeline has a total length of 2441km and a pipe diameter of 1219mm, with designed pressure of 12MPa and designed capacity of  $300 \times 10^8 \text{Nm}^3/\text{a}$ . There are 19 stations, of which 14 stations are equipped with 32 centrifugal compressors and 178 dry air coolers. Each air cooler is configured with two draught fans. The model of the dry air cooler installed is GP12×3-6-258-13.0S-S-23.4/DR-Ia. The geometry of the dry air cooler is shown in Figure 6.

#### 1) ACTUAL OPERATION SCHEME

The volume of distribution and injection of stations along the pipeline are displayed in Figure. 7 and schematic diagram of pipe network layout and pipe length between compressor stations are shown in Figure. 8. Moreover, the daily operation report of the pipeline on February 3, 2018, is shown in Table 2.

It can be seen from the report that the air coolers were not switched on in the actual operation scheme due to the low ambient temperature in February while there were 21 compressors being powered on. However, the natural gas outlet temperature is still high, leaving considerable room for

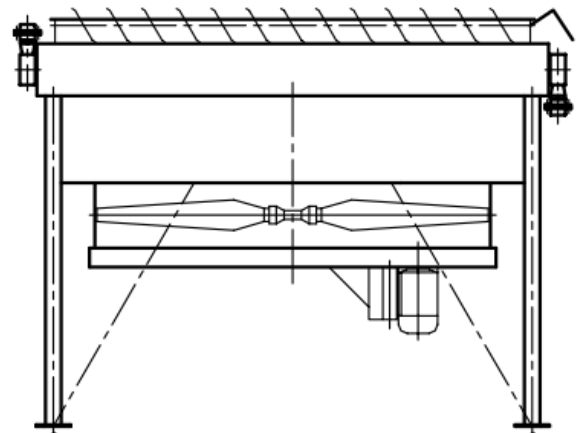


FIGURE 6. Air cooler geometry.

further optimization in terms of the number of power-on air coolers and energy consumption.

#### 2) OPTIMIZATION RESULT

As shown in Table 3, Table 4 and Table 5, these optimization schemes are obtained through the three algorithm solutions mentioned above.



TABLE 2. Daily operation report on February 3.

Station number	Pitted pressure (MPa)	Outbound pressure (MPa)	Pitted temperature (°C)	Outbound temperature (°C)	Number of power-on compressors	Compressor power (kW)	Unit efficiency (%)	Number of power-on air coolers	Air cooler power (kW)
1	7.62	9.42	20.37	38.45	2	46119.70	20.46	0	0
2	8.01	9.82	19.43	36.93	1	21955.41	20.10	0	0
3	8.93	9.62	8.34	30.86	1	17633.71	19.93	0	0
5	8.78	9.52	21.22	38.28	1	12667.37	20.57	0	0
7*	8.34	9.78	5.83	28.93	3	12654.63	67.23	0	0
9	8.94	11.16	24.72	37.12	2	44943.44	20.70	0	0
10	9.52	10.92	27.96	37.89	2	27721.76	22.15	0	0
12	8.92	11.05	22.80	36.09	1	21495.36	20.83	0	0
13	8.94	10.60	24.09	39.79	1	16965.01	21.24	0	0
14*	9.38	11.20	21.25	38.81	2	14986.16	74.87	0	0
15	9.45	11.03	19.95	31.09	1	15026.87	20.35	0	0
16	9.19	11.18	15.52	30.59	1	18595.03	21.57	0	0
17*	9.48	10.81	24.47	37.01	2	16977.84	68.22	0	0
19	8.08	11.16	21.61	38.76	1	11726.21	20.83	0	0

(Note: "\*" means that the compressor is electrically powered.)

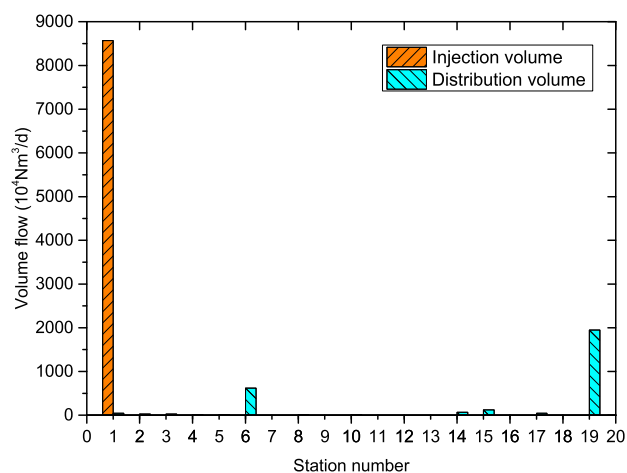


FIGURE 7. Schematic diagram: volume of distribution and injection.

Specifically, when adopting the GA method, there are three fewer power-on compressors and 63 more power-on air coolers in the optimized solution, compared to the actual operation scheme.

When it comes to the PSO method, there are one fewer power-on compressor and 58 more power-on air coolers in the optimized solution, compared to the actual operation scheme.

In regard to SA method, there are three fewer power on compressors and 93 more power-on air coolers in the optimized solution, compared to the actual operation scheme.

Therefore, it can be seen that the number of air coolers has increased and the number of compressors has reduced in the optimization schemes. Meanwhile, Figure. 9, Figure. 10 and Figure.11 show the differences between the actual operation scheme and these three algorithm solutions in the inlet and outlet pressure, outlet temperature and average efficiency of compressor units.

The total pressure drop between compressor stations can be calculated according to Figure. 9. Specifically, compared to

the total pressure drop of the actual operation scheme, that of GA, PSO and SA is 0.28MPa, 0.11MPa and 2.57 MPa lower respectively.

Further, since air coolers are switched off in winter, the outbound temperature is higher in the daily operation report. By contrast, more air coolers are designed to power on according to these three optimization solutions, leading to a marked decrease in outlet temperature in the solutions as shown in Figure. 10.

The average efficiency of compressors is compared in Figure. 11. It can be seen in these three solutions that there is a significant enhancement in the efficiency of diesel-powered and electric-powered compressor units, thus achieving the goal of energy conservation and consumption reduction.

### 3) ENERGY CONSUMPTION CALCULATION

Based on the energy consumption calculation method proposed in the previous studies [3], [4], various energy consumption indexes of each compressor station are calculated, such as the gas consumption, power consumption and production energy consumption, which lays a solid foundation for the comparison between the actual operation scheme and each optimization scheme as shown in Table 6. It can be concluded that there is the lowest production energy consumption in SA solution and therefore SA is crowned with the optimal scheme.

## B. DISCUSSION

### 1) COMPARATIVE ANALYSIS OF OPTIMIZATION ALGORITHMS

It is necessary to evaluate the advantages and disadvantages of an algorithm from two aspects: the optimization efficiency and the optimization quality, namely, the solution speed. Therefore, the optimization efficiency of the three optimization solutions, specifically, the solution time and the solution steps, are first compared, as shown in Figure. 12.

**TABLE 3. Optimized operation scheme (GA).**

Station number	Pitted pressure (MPa)	Outbound pressure (MPa)	Pitted temperature (°C)	Outbound temperature (°C)	Number of power-on compressors	Compressor power (kW)	Unit efficiency (%)	Number of power-on air coolers	Air cooler power (kW)
1	7.62	9.90	20.37	27.74	1	16790.62	20.88	8	512.92
2	8.26	10.31	16.06	29.32	1	13634.38	20.51	4	259.74
3	8.36	10.98	16.88	28.36	2	58134.1	20.34	7	453.56
5	9.37	10.56	8.85	13.52	1	11566.67	20.99	4	260.63
7*	8.76	10.44	9.95	19.72	2	17244.68	68.60	4	260.44
9	9.24	11.04	13.58	24.70	1	16944.35	21.12	4	256.04
10	9.52	11.10	19.91	27.64	1	14931.17	22.60	4	255.43
12	9.75	10.98	18.52	21.68	1	11196.12	21.26	4	259.05
13	9.15	11.01	12.58	24.96	1	17449.91	21.67	4	254.78
14*	9.75	10.88	15.76	20.13	2	20450.52	76.40	4	255.43
15	9.36	10.77	15.18	21.28	1	13051.25	20.77	4	258.61
16	9.51	10.82	9.00	16.51	1	16504.52	22.01	4	255.08
17*	9.05	10.82	13.43	24.78	2	22385.68	69.61	4	255.43
19	9.66	10.63	16.76	18.10	1	16320.59	21.25	4	259.18

**TABLE 4. Optimized operation scheme (PSO).**

Station number	Pitted pressure (MPa)	Outbound pressure (MPa)	Pitted temperature (°C)	Outbound temperature (°C)	Number of power-on compressors	Compressor power (kW)	Unit efficiency (%)	Number of power-on air coolers	Air cooler power (kW)
1	7.62	9.75	20.37	30.39	2	30098.64	20.67	6	384.69
2	8.04	10.04	17.10	30.17	1	13842.90	20.30	4	259.75
3	8.51	9.95	17.27	30.07	1	13262.94	20.14	4	259.18
5	8.11	10.76	9.12	29.11	1	19411.52	20.78	4	260.63
7*	8.91	10.68	18.85	27.47	2	21788.26	68.91	4	260.44
9	9.45	10.83	18.43	24.59	1	13112.99	20.91	4	256.04
10	9.57	10.79	19.84	27.41	2	29585.22	22.37	4	255.43
12	9.39	10.53	18.43	21.28	1	17772.29	21.05	4	259.05
13	8.69	10.55	12.40	25.67	1	18434.12	21.45	4	254.78
14*	9.19	10.94	16.08	26.53	3	29870.07	75.64	4	255.43
15	9.39	10.44	19.05	21.08	1	16726.89	20.56	4	258.61
16	9.11	10.58	8.95	18.52	1	13288.49	21.79	4	255.08
17*	8.82	9.70	14.66	17.92	2	17398.90	68.41	4	255.43
19	8.32	10.26	13.32	26.17	1	19585.98	21.04	4	259.18

**TABLE 5. Optimized operation scheme (SA).**

Station number	Pitted pressure (MPa)	Outbound pressure (MPa)	Pitted temperature (°C)	Outbound temperature (°C)	Number of power-on compressors	Compressor power (kW)	Unit efficiency (%)	Number of power-on air coolers	Air cooler power (kW)
1	7.62	9.59	20.37	23.50	1	18933.95	23.84	9	571.33
2	8.40	10.00	14.39	21.58	1	13846.85	23.49	8	505.64
3	8.54	10.04	13.32	20.40	1	17772.06	23.68	7	494.52
5	8.78	10.03	7.58	17.73	1	17133.70	21.36	5	312.55
7*	8.44	11.15	12.36	28.71	2	20012.42	71.24	7	433.09
9	10.01	10.51	19.21	12.20	1	12047.87	21.65	8	483.91
10	9.30	10.25	11.79	18.30	1	12180.73	24.03	4	282.30
12	8.91	10.27	15.00	15.12	1	13159.41	22.52	8	528.78
13	8.93	10.30	9.67	23.11	1	16404.46	23.81	5	293.26
14*	8.91	10.70	14.91	24.82	3	31141.89	69.86	5	315.27
15	9.43	10.35	18.01	15.17	1	11326.35	22.49	8	526.59
16	9.24	10.43	7.51	19.57	1	11428.44	21.60	10	659.71
17*	8.98	11.06	9.17	26.53	2	20406.70	70.12	4	284.36
19	9.23	10.38	17.64	12.32	1	16305.08	23.49	5	330.76

It can be seen from Figure. 12 that GA converges in 240 steps, which takes 106.64s and PSO converges in 480 steps, which takes 207.05s. However, SA converges in 3158 steps

(convergence is not indicated in Figure. 12 due to a large number of steps), which takes 231.51s. Although its optimization scheme is considered the best solution of the three,

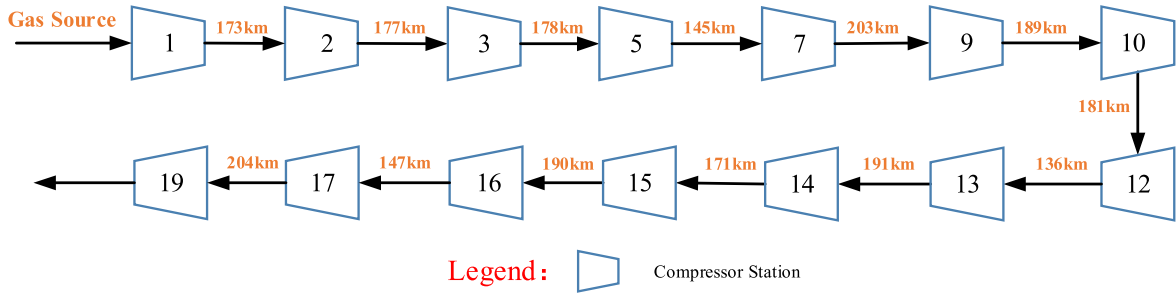


FIGURE 8. Schematic diagram of pipe network layout.

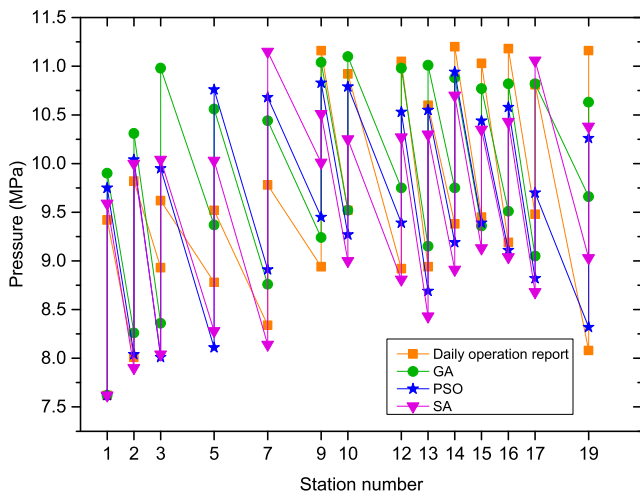


FIGURE 9. Comparison of inlet and outlet pressure of each compressor station.

TABLE 6. Comparison of monthly energy consumption indicators.

Energy consumption index	Actual operation plan	Optimized operation plan		
		GA	PSO	SA
Solution time (s)		106.64	207.05	231.51
Turnover ( $10^7 \text{Nm}^3 \cdot \text{km}$ )		581089.46		
Gas consumption ( $10^4 \text{Nm}^3$ )	9292.30	7530.23	7479.13	5853.54
Power consumption ( $10^4 \text{kW} \cdot \text{h}$ )	3212.54	4617.88	5240.95	5585.98
Total energy consumption (tce)	127535.80	105827.43	105913.56	84717.25

its calculation steps can take such a long time, resulting in lower optimization efficiency.

Further, optimization quality can be compared based on the energy consumption indexes of different optimization algorithms above. With total energy consumption indexes in Figure. 13, the merits and drawbacks of the optimization results of different optimization algorithms for the calculation example in this research can be more visualized.

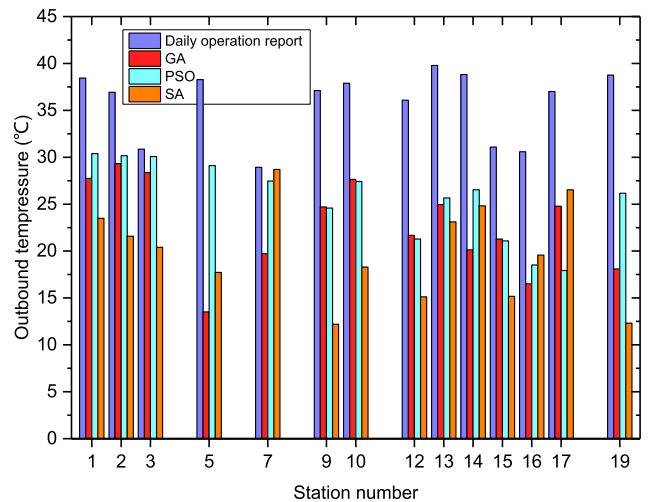


FIGURE 10. Comparison of the outbound temperature of each compressor station.

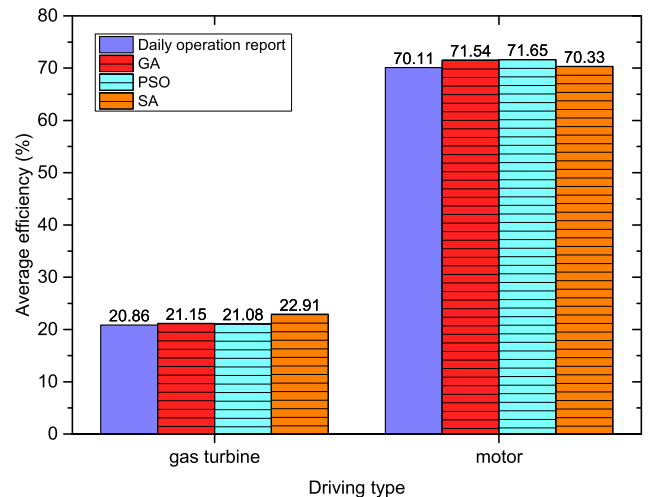


FIGURE 11. Comparison of average efficiency of compressor units.

It can be concluded from Figure. 13 that the three algorithm optimization schemes all reduce the total production energy consumption, while there is also a marked decline in the gas consumption of the diesel-powered compressors.

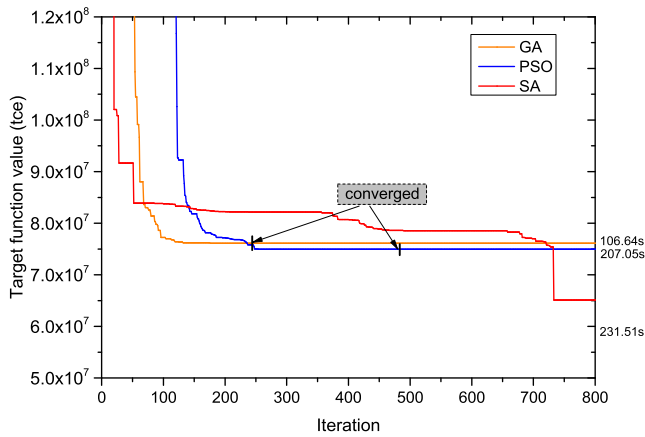


FIGURE 12. Comparison of solution time and solution steps of different algorithms.

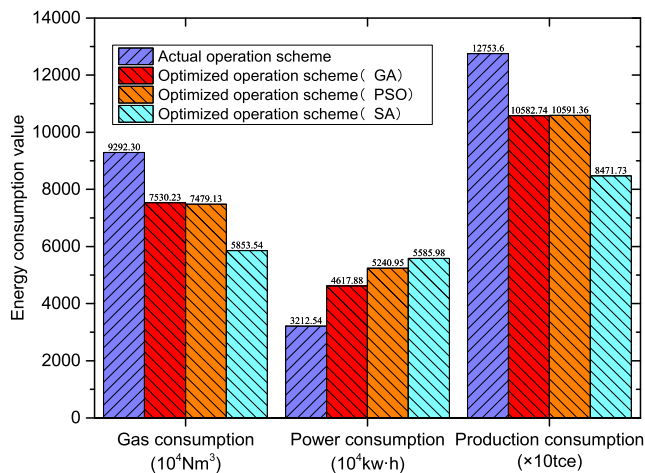


FIGURE 13. Comparison of total energy consumption of different algorithms in February 2018.

Nevertheless, the power consumption is slightly ascending compared with the actual operation scheme due to the increased number of power-on air coolers in the optimization schemes. After converting power consumption and gas consumption into standard coal consumption, the total production energy consumption is still much lower than that in the actual operation scheme. Specifically, SA optimization scheme reduces the production energy consumption by 17.02%, PSO optimization scheme by 16.95% and SA optimization scheme by 33.57%. Therefore, the energy consumption is greatly decreased in these three optimization solutions.

In general, the optimized operation schemes solved by the three algorithms reduce the gas consumption and the number of power-on compressors. However, these solutions increase the power consumption due to more power-on air coolers to lower the outlet temperature of some compressor stations, so as to reduce the friction loss of pipelines in the latter sections, the pressure head required by the compressors and the gas consumption. Therefore, it can be concluded from the optimization results that optimized operation schemes that

take air coolers into account can significantly lower the total production energy consumption of the compressor stations of the long-distance natural gas pipeline, which proves the optimization objective is correct and practical.

## 2) ANALYSIS ON THE BEST TIMING TO POWER ON AIR COOLERS

The heat transfer mechanism of air coolers is the heat exchange between the cold air and the high-temperature natural gas through finned tubes, and hence the air temperature casts direct influence on the cooling effect of air coolers. Further, given annual temperature of stations along the pipeline ranging from below  $-18^{\circ}\text{C}$  to above  $30^{\circ}\text{C}$ , when to power on air coolers for greater economic benefits is the most concerned issue of the station management department. Therefore, the air temperature is considered an optimization variable in this research in order to find out the most suitable air temperature for each compressor station to turn on its air coolers. As shown in Figure. 14, the total energy consumption of the compressor units across the pipeline  $\sum_{i=1}^n N_{compressor,i}$  is calculated with all air coolers switched off, and the total energy consumption of the compressor units and the air cooler units across the pipeline  $\sum_{i=1}^n (N_{compressor,i} + N_{aircooler,i})$  are also computed with all air coolers powered on. With the annual air temperature range of each compressor station as the upper and lower limits, these three optimization algorithms can provide a temperature solution when  $\sum_{i=1}^n (N_{compressor,i} + N_{aircooler,i}) - \sum_{i=1}^n N_{compressor,i} \leq 0$ . If the air temperature is lower than this optimized temperature, turning on the air coolers can be well advised to reduce the energy consumption of the entire pipeline.

In Figure.14:  $N_{compressor,n}$ — compressor energy consumption of compressor station  $n$ , tce;

$N_{aircooler,n}$ — air cooler energy consumption of compressor station  $n$ , tce;

$T_{summer,n}$ — summer air temperature of compressor station  $n$ ,  $^{\circ}\text{C}$ , in which  $T_{s\min,n}$  is the lowest temperature in summer and  $T_{w\max,n}$  is the highest temperature in summer;

$T_{winter,n}$ — winter air temperature of compressor station  $n$ ,  $^{\circ}\text{C}$ , in which  $T_{w\min,n}$  is the lowest temperature in winter and  $T_{w\max,n}$  is the highest temperature in winter;

It is displayed in Figure.15 and Figure.16 about the temperatures of each compressor station suitable for switching on air coolers in winter and summer. It can be seen that these temperatures recommended by the three algorithms are approximate, which proves that the calculation results are accurate. Moreover, due to the lower temperature in winter, the cooling effect after turning on the air coolers is better, and hence the energy consumption can be greatly reduced. Therefore, when the temperature is below the optimal temperature curve, powering on air coolers can be more likely to reduce the energy consumption of the whole pipeline. Comparatively,

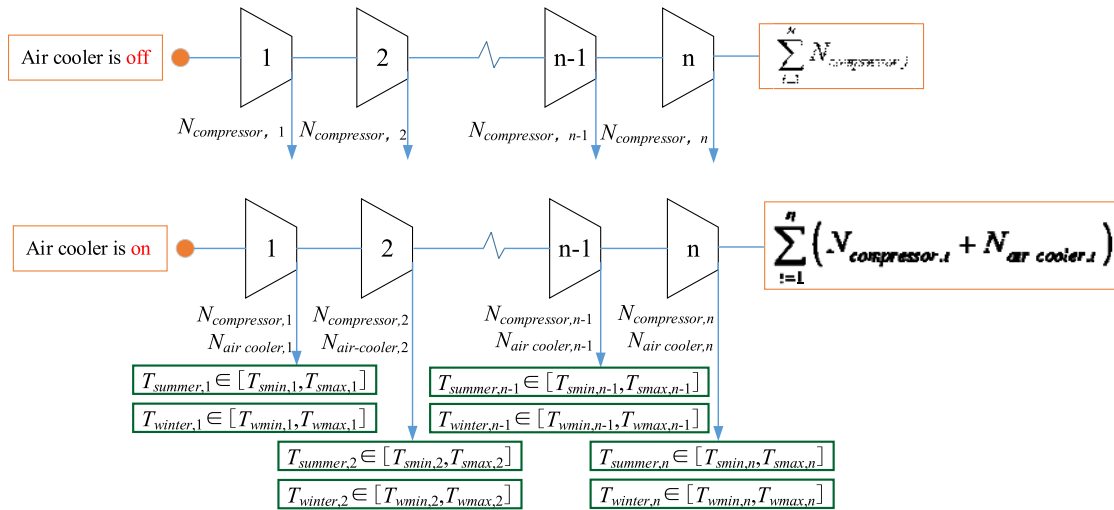


FIGURE 14. Schematic diagram: energy consumption changes for powering on air cooler.

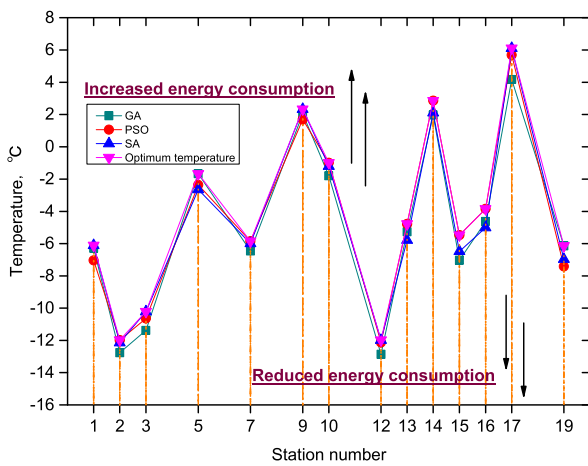


FIGURE 15. Temperature comparison of powering on air coolers in each compressor station in winter.

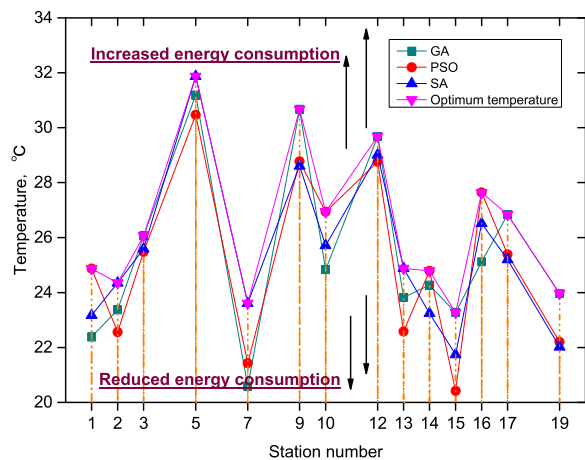


FIGURE 16. Temperature comparison of powering on air coolers in each compressor station in summer.

while the temperature is above the optimal temperature curve, the cooling effect is poorer, which can increase the total energy consumption. As a result, given higher air temperature

and outlet temperature of natural gas in summer, if the air temperature is below the optimal temperature curve, it is well advised to power on air coolers for energy consumption reduction of the pipeline, otherwise it may increase energy consumption if the air temperature is above the curve. For this reason, it is suggested to turn on the air coolers when the air temperature is below the temperature curves as shown in Figure. 15 and Figure. 16, so as to lower energy consumption and obtain greater economic benefits.

IV. CONCLUSION

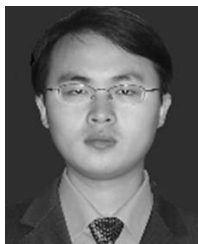
(1) In the gas transmission pipeline system, the compressors, air coolers, and pipelines are coupled and interacted with each other. The innovation of this research is to set up an optimization model for the combined operation of air coolers and compressors with the goal of achieving lowest energy consumption. By optimizing the scheme of powering on compressors and air coolers, the production energy consumption can be significantly reduced, which is of great application value.

(2) Given the direct influence of air temperature on the cooling effect of air coolers and the tremendous variation of annual air temperature of stations along the pipeline, when to power on air coolers for greater economic benefits is the most concerned issue of the station management department. For this reason, this research proposes to take the air temperature as an optimization variable to seek for and optimize the most suitable air temperature for each compressor station to switch on its air coolers. Such a solution can serve as an optimal guide on the pipeline operation for further promotion and broader use.

(3) A comparison of GA solution, PSO solution, and SA solution has been carried out in this research. Specifically, GA solution boasts the fastest solution speed while even though being the slowest, SA solution provides the best optimization result.

## REFERENCES

- [1] Z. Su, E. Liu, and Y. Xu, "Flow field and noise characteristics of manifold in natural gas transportation station," *Oil Gas Sci. Technol.*, vol. 74, pp. 1–9, 2019. doi: 10.2516/ogst/2019038.
- [2] H. Lu, K. Huang, and M. Azimi, "Blockchain technology in the oil and gas industry: A review of applications, opportunities, challenges, and risks," *IEEE Access*, vol. 7, pp. 41426–41444, 2019.
- [3] P. Xie, Q. Wang, and S. Wang, "Analysis of natural gas pipeline running in winter," *Pipeline Technol. Equip.*, no. 2, pp. 67–69, Mar. 2015.
- [4] K. Chi, U. Varanon, W. Christine, W. Chen, and P. Tontiwachwuthikul "An Integrated expert system/operations research approach for the optimization of natural gas pipeline operations," *Eng. Appl. Artif. Intel.*, vol. 13, no. 4, pp. 465–475, Aug. 2000.
- [5] E. Liu, C. Li, and Y. Yang, "Optimal energy consumption analysis of natural gas pipeline," *Sci. World J.*, vol. 2014, May 2014, Art. no. 506138.
- [6] E. Liu, L. Lv, Q. Ma, J. Kuang, and L. Zhang, "Steady-state optimization operation of the west-east gas pipeline," *Adv. Mech. Eng.*, vol. 11, no. 1, pp. 1–14, Jan. 2019.
- [7] A. Demissie, W. Zhu, and C. Belachew, "A multi-objective optimization model for gas pipeline operations," *Comput. Chem. Eng.*, vol. 100, pp. 94–103, May 2017.
- [8] I. E. Ghoujdi, H. Hadiannasab, M. Bidi, A. Naeimi, M. H. Ahmadi, M. A. Nazari, and T. Ming, "Multiobjective optimization design of the solar field and reverse osmosis system with preheating feed water using Genetic algorithm," *Energy. Sci. Eng.*, vol. 6, no. 6, pp. 624–642, Dec. 2018.
- [9] R. Z. Ríos-Mercado and C. Borraz-Sánchez, "Optimization problems in natural gas transportation systems: A state-of-the-art review," *Appl. Energ.*, vol. 147, pp. 536–555, Jun. 2015.
- [10] K. Kazda and X. Li, "Approximating nonlinear relationships for optimal operation of natural gas transport networks," *Processes*, vol. 6, no. 10, p. 198, Oct. 2018.
- [11] Z. Yang, B. Zhang, and W. Liu, "Air cooler transformation technology innovation," *Mech. Eng.*, no. 11, pp. 164–166, May 2016.
- [12] M. Mikolajkova, H. Saxén, and F. Pettersson, "Linearization of an MINLP model and its application to gas distribution optimization," *Energy*, vol. 146, pp. 156–168, Mar. 2018.
- [13] S. Wu, R. Z. Ríos-Mercado, E. A. Boyd, and L. R. Scott, "Model relaxations for the fuel cost minimization of steady-state gas pipeline networks," *Math. Comput. Model.*, vol. 31, nos. 2–3, pp. 197–220, Jan./Feb. 2000.
- [14] T. W. K. Mak, P. Van Hentenryck, A. Zlotnik, and R. Bent, "Dynamic compressor optimization in natural gas pipeline systems," *Inform. J. Comput.*, vol. 31, no. 1, pp. 40–65, Jan. 2019.
- [15] D. E. Goldberg, "Computer-aided gas pipeline operation using genetic algorithms and rule learning part II: Rule learning control of a pipeline under normal and abnormal conditions," in *Proc. PSIG Annu. Meeting*, Albuquerque, USA, 1985, p. 3174. [Online]. Available: <https://link.springer.com/article/10.1007/BF01198148>
- [16] A. Konak, D. W. Coit, and A. E. Smith, "Multi-objective optimization using genetic algorithms: A tutorial," *Rel. Eng. Syst. Saf.*, vol. 91, no. 9, pp. 992–1007, Sep. 2006.
- [17] S. Sanaye and J. Mahmoudimeh, "Minimization of fuel consumption in cyclic and non-cyclic natural gas transmission networks: Assessment of genetic algorithm optimization method as an alternative to non-sequential dynamic programming," *J. Taiwan. Inst. Chem. E.*, vol. 43, no. 6, pp. 904–917, Nov. 2012.
- [18] J. Kennedy, "Particle Swarm Optimization," in *Proc. Encyclopedia Mach. Learn.*, 2010, pp. 760–766.
- [19] L. G. Li, Z. H. Zhang, and Y. S. Dai, "Operation optimization based on improved pattern search algorithm in gas transmission networks," *J. China University Petroleum*, vol. 36, no. 4, pp. 139–143, Apr. 2012.
- [20] M. Zhou, Y. Zhang, and S. Jin, "Dynamic optimization of heated oil pipeline operation using PSO-DE algorithm," *Measurement*, vol. 59, pp. 344–351, Jan. 2015.
- [21] M. R. Javadi, K. Mazlumi, and A. Jalilvand, "Application of GA, PSO and ABC in optimal design of a stand-alone hybrid system for north-west of Iran," in *Proc. 7th Int. Conf. Elect. Electron. Eng.*, Bursa, Turkey, Dec. 2011, pp. 204–211.
- [22] A. Marzoughi, H. Selamat, and F. Marzoughi, "Application of particle swarm optimization approach to improve PID performance for a gas turbine temperature control system," in *Proc. 8th IEEE Student Conf. Res. Develop.*, Putrajaya, Malaysia, Dec. 2010, pp. 224–229.
- [23] S. Kirkpatrick, J. Gelatt, and M. P. Vecchi, "Optimization by simulated annealing," *Science*, vol. 220, no. 4598, pp. 671–680, May 1983.
- [24] Z. Huaixin, Y. Yi, and L. Ming, "Optimization of large-scale natural gas pipeline network base on the combined GASA algorithm," in *Proc. Int. Conf. Comput. Informat. Sci.*, Chengdu, China, Dec. 2010, pp. 254–257.
- [25] A. Chebouba, F. Yalaoui, L. Amodeo, A. Smati, and A. Tairi "New method to minimize fuel consumption of gas pipeline using ant colony optimization algorithms," in *Proc. Int. Conf. Service Syst. Service Manage.*, Troyes, France, Oct. 2006, pp. 947–952.
- [26] A. Chebouba and H. Megloul, "A new combined artificial neural networks and ant colony optimization algorithm for energy minimization in pipeline operations," in *Proc. 3rd Int. Conf. Ind. Eng. Oper. Manag.*, Istanbul, Turkey, 2012, pp. 1–10.
- [27] W. Liu, M. Li, Y. Liu, Y. Xu, and X. Yang, "Decision of optimal scheduling scheme for gas field pipeline network based on hybrid genetic algorithm," in *Proc. 1st ACM/SIGEVO Summit Genetic Evol. Comput.*, Shanghai, China, Jun. 2009, pp. 369–374.
- [28] M. MohamadiBaghmolaei, M. Mahmoudy, and D. Jafari, R. MohamadiBaghmolaei, and F. Tabkhi, "Assessing and optimization of pipeline system performance using intelligent systems," *J. Nat. Gas Sci. Eng.*, vol. 18, pp. 64–76, May 2014.
- [29] W. Qiao, B. Chen, and S. Wu, "A forecasting model of natural gas daily load based on wavelet transform and LSSVM—DE," *Natural Gas Ind.*, vol. 34, no. 9, pp. 118–124, Sep. 2014.
- [30] C. Borraz-Sánchez and R. Z. Ríos-Mercado, "Improving the operation of pipeline systems on cyclic structures by tabu search," *Comput. Chem. Eng.*, vol. 33, no. 1, pp. 58–64, Jan. 2008.
- [31] P. Wong and R. Larson, "Optimization of natural-gas pipeline systems via dynamic programming," *IEEE Trans. Autom. Control*, vol. AC-13, no. 5, pp. 475–481, Oct. 1968.
- [32] D. Danilovic, V. K. Maricic, and I. Ristovic, "Determination of optimal parameters of distributive gas pipeline by dynamic programming method," *Petrol. Sci. Technol.*, vol. 29, no. 9, pp. 924–932, Mar. 2011.
- [33] H. A. Behrooz and R. B. Boozarjomehry, "Dynamic optimization of natural gas networks under customer demand uncertainties," *Energy*, vol. 134, pp. 968–983, Sep. 2017.
- [34] E. Liu, W. Li, H. Cai, and S. Peng, "Formation mechanism of trailing oil in product oil pipeline," *Processes*, vol. 7, no. 1, pp. 1–18, Jan. 2019.
- [35] L. Lv, "Study on optimization of combined operation of air cooler and compressor in pipeline system of west section of west second line," M.S. thesis, School Petroleum Natural Gas Eng., Southwest Petroleum Univ. Chengdu, China, 2019.
- [36] E. Liu, C. Li, L. Yang, S. Liu, M. Wu, and D. Wang, "Research on the optimal energy consumption of oil pipeline," *J. Environ. Biol.*, vol. 36, pp. 703–711, Jul. 2015.
- [37] D. Ma, W. Tan, Q. Wang, Z. Zhang, J. Gao, Q. Zeng, X. Wang, F. Xia, and X. Shi, "Application and improvement of swarm intelligence optimization algorithm in gas emission source identification in atmosphere," *J. Loss Prevention Process Ind.*, vol. 56, pp. 262–271, Nov. 2018.
- [38] H. Zhang, Y. Liang, J. Ma, Y. Shen X. Yan, and M. Yuan, "An improved PSO method for optimal design of subsea oil pipelines," *Ocean. Eng.*, vol. 141, pp. 154–163, Sep. 2017.
- [39] B. Dantas and E. Cáceres, "An experimental evaluation of a parallel simulated annealing approach for the 0–1 multidimensional knapsack problem," *J. Parallel Distrib. Comput.*, vol. 120, pp. 211–221, Oct. 2018.
- [40] A. Rodríguez, P. P. Oteiza, and N. B. Brignole, "Simulated annealing optimization for hydrocarbon pipeline networks," *Ind. Eng. Chem. Res.*, vol. 52, no. 25, pp. 8579–8588, May 2013.
- [41] I. Samora, M. J. Franca, A. J. Schleiss, and H. M. Ramos, "Simulated annealing in optimization of energy production in a water supply network," *Water. Resour. Manag.*, vol. 30, no. 4, pp. 1533–1547, Mar. 2016.
- [42] C. Li, "Gas pipeline thermal calculation," in *Natural gas pipeline transportation*, 2nd ed. Beijing, China, Petroleum, press, 2008, pp. 97–100.
- [43] M. Chaczykowski, and A. J. Osiadacz, "Comparative assesment of steady-state pipeline gas flow models," *Arch. Min. Sci.*, vol. 57, no. 1, pp. 23–38, Oct. 2012.
- [44] K. Gersten, H. D. Papenfuss, T. Kurschat, P. Genillon, F. F. Perez, and N. Revell, "Heat transfer in gas pipelines," *OIL. Gas-Eur. Mag.*, vol. 27, no. 1, pp. 30–34, Mar. 2001.
- [45] E. Liu, X. Ma, and M. Zhou, "Analysis of discharge process of oil pipeline with complex topography," *Energy Rep.*, vol. 5, pp. 678–687, Jun. 2019.



**ENBIN LIU** received the B.S. and M.S. degrees in oil-gas storage and transportation engineering from Southwest Petroleum University, in 2003 and 2005, respectively, where he is currently a Professor with the Petroleum Engineering School. His research interests include oil and gas pipeline network simulation and optimization technology, transient flow, and computational fluid dynamics.



**YANG YI** received the B.S. degree in mechanical and the M.S. degree in oil-gas storage and transportation engineering from Southwest Petroleum University, in 2016 and 2019, respectively. His research interests include oil and gas pipeline network simulation and optimization technology, and computational fluid dynamics.



**LIUXIN LV** received the B.S. degree in oil-gas storage and transportation engineering from Changzhou University, in 2016, and the M.S. degree in oil-gas storage and transportation engineering from Southwest Petroleum University, in 2019. His research interests include gas pipeline network simulation and optimization technology, and computational fluid dynamics.



**PING XIE** received the B.S. degree in oil-gas storage and transportation engineering from the China University of Petroleum, in 1997, and the M.S. degree in oil-gas storage and transportation engineering from Southwest Petroleum University, in 2012. She is currently an Engineer with Petrochina Northwest United Pipeline Company Ltd. Her research interest includes safe and economic transportation of oil and gas pipelines.

...